Separation Science and Technology
Publication details, including instructions for authors and subscription information:
http://www.informaworld.com/smpp/title~content=t713708471

Cross-Flow Microfiltration of Oily Water using a Ceramic Membrane: Flux Decline and Oil Adsorption

Shingjiang Jessie Lue[a]; Jayin Chow[a]; Chinfeng Chien[a]; Hsengshao Chen[a]
[a] Department of Chemical and Materials Engineering and Green Technology Research Center, Chang Gung University, Kwei-shan, Taoyuan County, Taiwan

To cite this Article Lue, Shingjiang Jessie , Chow, Jayin , Chien, Chinfeng and Chen, Hsengshao(2009) 'Cross-Flow Microfiltration of Oily Water using a Ceramic Membrane: Flux Decline and Oil Adsorption', Separation Science and Technology, 44: 14, 3435 — 3454
To link to this Article: DOI: 10.1080/01496390903212714
URL: http://dx.doi.org/10.1080/01496390903212714

Separation Science and Technology, 44: 3435–3454, 2009

ISSN: 0149-6395 print/1520-5754 online
DOI: 10.1080/01496390903212714

Taylor & Francis
Taylor & Francis Group

Cross-Flow Microfiltration of Oily Water using a Ceramic Membrane: Flux Decline and Oil Adsorption

Shingjiang Jessie Lue, Jayin Chow, Chinfeng Chien, and Hsengshao Chen
Department of Chemical and Materials Engineering and Green Technology Research Center, Chang Gung University, Kwei-shan, Taoyuan County, Taiwan

Abstract: The microfiltration of oil-water emulsion solutions through a ceramic membrane was investigated in this study. A surfactant-free dispersed oil-water emulsion in the range of 0.2–2% kerosene was fed into a tubular ceramic membrane module as a turbulent flow. The optimal trans-membrane pressure was determined. For oily water containing less than 0.5% kerosene content, the steady-state permeate flux of $3.36 \times 10^{-5}\,m^3/m^2\,s$ bar ($121\,L/m^2\,h$ bar) could be achieved; the oil retention was as high as 99.5% at a volume concentration factor of 4. The solute diffusion coefficient was $9.765 \times 10^{-10}\,m^2/s$ and the mass transfer coefficient was $2.687 \times 10^{-5}\,m/s$ in this system. The resistance-in-series model was applied to describe the flux decline and the individual resistance from the membrane, oil adsorption, gel formation, and concentration polarization were calculated. The results indicated that the oil (solute) adsorption on the membrane surface was the major source of resistance. The scanning electron micrograph indicated oil adsorption on the membrane surface. As the oil content in the feed increased, the gel formation and the concentration polarization also played a role, contributing to flow resistance and causing flux decline. Furthermore, increasing the operating temperature enhanced the flux and the activation energy was determined as 2.918 kJ/mol. A reversible model of dispersed oil adsorption into the gel state was used to explain the flux decline during the filtration process.

Received 4 November 2008; accepted 2 July 2009.
Address correspondence to Shingjiang Jessie Lue, Department of Chemical and Materials Engineering, Chang Gung University, Kwei-shan, Taoyuan County, Taiwan, 333. Tel.: +886-3-2118800 Ext. 5489; Fax: +886-3-2118700. E-mail: jessie@mail.cgu.edu.tw

Keywords: Ceramic membrane, flux decline, microfiltration, modeling, oil-water separation

INTRODUCTION

Many industrial wastewaters contain oily components. Metal fabrication, food processing, gas and oil industries are the major sources of oily wastewater. The oils and greases in the wastewater must be removed before discharge into sewers or open water storage. Regulations require that the maximum oil concentration in discharge water be 5–40 ppm (1,2). This standard is rarely achieved by conventional methods, e.g., chemical treatment, gravity settling, adsorption, and biological decomposition. Membrane separation, however, seems to be a suitable technology for oil-water separation. It possesses the distinct advantages of reduced sludge, high quality permeate water, ease of operation, small space requirement, and the possibility of recycling treated water. It can also recover or concentrate the oily components for reuse or incineration. These features make membrane separation an environmentally-friendly process.

Lee et al. (3) first used polymeric ultrafiltration membranes to study the concentration polarization and fouling phenomena in soluble oil systems. They found that the rejected oil formed a gel layer of 40% oil content on the membrane surface. Since then, many researchers have used ultrafiltration membranes to retain oily components from wastewater and produced clean, low oil content permeates (2,4–6). The oil droplet size was usually in the micrometer range and ultrafiltration, or even microfiltration, membranes can sufficiently remove oily constituents based on the sieving mechanism. Although hydrophobic ultrafiltration membranes were tested extensively, the hydrophilic surface has shown to decrease oil adsorption and inhibit fouling during the filtration processes (7–9). Up to now, micro- and ultrafiltration polymeric membranes were investigated to treat oily wastewater from the metal industry (5,10), soybean oil processing (11), heavy crude oil, and oilfield brines (12–14). The oil rejection was generally high, in the 94–99% range (10,12,15). The permeate flux, however, declined substantially after a short period of operation. A flux reduction of 90% from the initial flux was not uncommon (12). A low permeate flux has a negative impact on the feasibility and economics of the membrane process and, therefore, its occurrence must be prevented or minimized.

Recently, with the development of ceramic membranes, researchers found applications for treating oil-water systems using ceramic membranes (2,12–14,16–20). The advantages associated with ceramic

membranes, such as resistance to fouling, ease of cleaning, high tolerance for a wide range of the pH, and the temperature, make ceramic membranes superior to their polymeric counterparts (5,16). Although the permeate flux on ceramic membranes is higher than the polymeric membranes, the flux decline is still inevitable. It is noted that concentration polarization, membrane fouling, membrane blocking, etc., can cause the flux decline. The fouling and blocking mechanisms for oily wastewater in micro/ultrafiltration are still not well understood. Belfort et al. (21) presented a thorough review of the flow behavior of suspensions and macromolecular solutions in crossflow microfiltration. Koltuniewicz and Field (5) proposed a model based on the pore blocking theory to predict flux at various elapsed times using 0.1 μm ceramic membranes. Elmaleh and Ghaffor (2) used dimensionless analysis to establish fouling resistance for ceramic ultrafiltration membranes.

The objective of this study was to determine the permeation flux, the separation efficiency, and the oil adsorption mechanism in the microfiltration of oil-water mixtures using a tubular ceramic membrane. A micro-filter instead of an ultrafiltration membrane was used in an attempt to enhance the permeate permeability (14). The process was carried out in a batch mode at a constant concentration and also in a concentration mode. The oil retention and flux were determined at various volume concentration factors (VCF). Attention was focused on the various resistance components that caused the flux decline. The effect of operating conditions (oil concentration, temperature, volume concentration factor) on water flux was determined.

MATERIALS AND METHODS

Membrane Operation

A surfactant-free dispersed kerosene-water mixture was prepared by mixing kerosene (Chinese Petroleum Corp., Taiwan) and high purity deionized water (produced by models RiOs-5 and Milli-Q Gradient, Millipore Corp., Bedford, Massachusetts, USA). The oil concentration in the feed emulsion ranged from 0.2 to 2% (w/w) and the feed weighed ca. 4 kg. The kerosene-water emulsion was continuously mixed using a stirrer (model HC-100 A, 100 W power, Ho-Chen Co., Taiwan) with an impeller $\phi 80\,\text{mm} \times 500\,\text{mm}$. The impeller's rotational speed was adjusted to a speed of 2000–3000 rpm, which was sufficiently high to maintain a homogeneous dispersion of oil but not to entrain air into

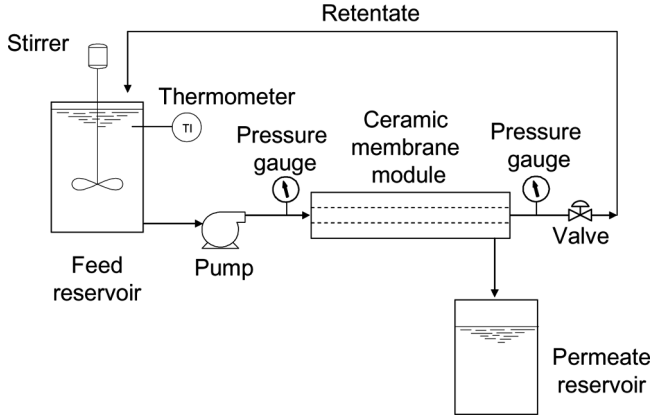

Figure 1. Experimental set-up of microfiltration of the kerosene-water mixture.

the solution. The oil-water solution in the mixing tank was fed into a tubular ceramic membrane module using a diaphragm pump (model TYP 2500, Deng Yuan Co., Taiwan) as shown in Fig. 1. Table 1 shows the characteristics of the ceramic membrane and the module (membrane type M14, Micro Carbosep^{TM} 40, Tech-Sep, Rhône-Poulenc Group, Miribel Cedex, France). The capacity of the feed pump was determined at 16.6 cm^3/s of water. The unused, brand new membrane was first soaked in a 30% nitric acid (reagent grade, Shimakyu's Pure Chemicals, Osaka, Japan) solution to remove the impurities. The membrane was then rinsed with tap water and deionized water. To measure the water permeability of the membrane, deionized water at 20°C was fed into the membrane module and a flux-operating pressure relationship was established. The pure water flux was used to calculate the hydrodynamic resistance of the membrane (R_m) as well as an indication of the cleaning efficiency after each run.

The oil-water mixture microfiltration process was first carried out in a batch mode at constant feed composition. Both the retentate and the permeate were recycled into the feed tank. The operation pressure was selected randomly and the permeate flux was determined by weighing the permeate for one minute. A flux-operation pressure relationship was thus established. When the flux reached a "plateau" with the increasing pressure, the flux was referred to as the limiting flux (J_∞). The oil content effect on J_∞ could be obtained and the mass transfer parameters—mass transfer coefficient (k), diffusion coefficient (D), and boundary layer thickness (δ) were calculated as described in the concentration model (22).

Table 1. Characteristics of the ceramic membrane used in this study

Module	
Outer diameter (mm)	17/38
Length (mm)	475
Net weight (kg)	1.1
Material	stainless steel 316 L
Internal Volumes	
Retentate side (ml)	15
Permeate side (ml)	17
Membrane	
Outer diameter (mm)	10
Inner diameter (mm)	6
Length (mm)	400
Membrane surface area (m^2)	0.0075
Pore size (μm)	0.14
Membrane material	
Support	Carbon
Separation layer	ZrO_2-TiO_2 on inner wall
Operating Parameters	
pH	1∼14
Lowest temperature (°C)	1
Max. process temp. (°C)	95
Max. cleaning temp. (°C)	85
Operating pressure (bar)	0 ∼ 14
Max. differential pressure (bar)	4
Chemical sterilization	yes

The flux decline behaviors at various oil concentrations were then determined. Again the retentate and the permeate were recycled into the feed reservoir to keep the feed composition constant. The initial flux (J_o), flux at steady state (J_{ss}) and the flux history were recorded using the optimal operating pressure, determined previously. The J_{ss} data were used to determine the various resistances under steady state as described in the following section.

The emulsion was finally concentrated by recycling only the retentate. The extent of concentration was expressed in volume concentration factor (VCF), which is defined as the volume of the initial feed to final volume. After reaching a VCF of 1.5, 2, 3, and 4, sample aliquots were taken from the permeate reservoir for oil content determination. The overall oil retention (R) was calculated as $(1-V_pC_P/V_FC_F) \times 100\%$, %, where V_p, V_F, C_P, and C_F were the volume of the permeate and the feed, and the oil concentration in the permeate and in the initial feed, respectively.

Cleaning of the Membrane

After each run, the membrane was removed from the module housing and soaked in a 30% NaOH (Shimakyu's Pure Chemicals, Osaka, Japan) solution for 12 hours. The membrane was rinsed with tap water, followed by rinsing with deionized water of about two liters, to remove the alkali solution. The membrane was then soaked in a 30% nitric acid (Shimakyu's Pure Chemicals, Osaka, Japan) solution for more than 12 hours. Tap water and deionized water were used to rinse the nitric acid away. The membrane was installed into the housing and 4-L deionized water was pumped into the membrane system to clean the membrane, the module, the tubing, and the fitting. To ensure that the cleaning was completed, the pH value of the permeate was checked and the water permeate flux was recorded. The pH of the permeate should be the same as that of the deionized water, and the water flux cannot deviate more than 5% from the water permeability determined on an unused clean membrane, as determined previously. After assuring that the membrane was clean and the water flux was restored, the membrane was installed into the housing, ready for the next run.

Oil Content Measurement

The oil concentration in the permeate was determined using a modified method from Gu et al. (23). Fifty milliliters of oil-water emulsion was mixed with 50 ml of reagent grade petroleum ether (Acros Organics, Fisher Scientific, Pittsburgh, Pennsylvania, USA). The mixture was allowed to stand for 15 minutes and the upper layer phase was taken for the oil content analysis using an ultraviolet-visible (UV-VIS) spectrophotometer (Cary 1E, Varian Instruments, Palo Alto, California, USA).

The calibration curve was established in a similar manner. Five standard solutions were prepared by mixing kerosene of known volume with petroleum ether. The standard solutions were scanned at a wavelength between 235 and 300 nm and the absorbance at a local maximum wavelength (λ_{max}) was recorded. A straight regression line of absorbance vs. the kerosene content was generated using the least squares method.

Resistance-In-Series Model

The effect of various resistance sources on the permeate flux under steady state was proposed using a resistance-in-series model. Mulder (22)

states that the flux decrease can be caused by several factors, such as concentration polarization, adsorption, gel layer formation, and the plugging of the pores. Together with the resistance caused by the membrane, the total resistance towards mass transport across a membrane is the summation of R_p, R_a, R_m, R_g, and R_{cp}, which represents the resistance caused by pore-blocking, adsorption, membrane, gel layer formation and concentration polarization, respectively. Various resistances contribute to a different extent to the total resistance, R_{tot}. According to the resistance model theory, the flux through a membrane can be expressed as:

$$flux = \frac{driving\ force}{viscosity \cdot total\ resistance} \tag{1}$$

In the pressure-driven membrane process, Eq. (1) can be rewritten as:

$$J = \frac{\Delta P}{\eta \cdot R_{tot}} \tag{2}$$

where η is the viscosity of the feed and

$$R_{tot} = R_m + R_a + R_p + R_g + R_{cp} \tag{3}$$

wherever applicable.

In the case of microfiltration of pure water through a clean membrane, the membrane resistance (R_m) can be determined from the pure water flux (J_w) through a clean membrane according to:

$$J_w = \frac{\Delta P}{\eta \cdot R_m} \tag{4}$$

In estimating R_a, the clean membrane was immersed in a kerosene emulsion of known oil concentration until an equilibrium condition was reached. The membrane with the adsorbed solute was installed in the housing and pure water flux was measured again. The initial water flux through the solute-adsorbed membrane (J_{wa}) should be:

$$J_{wa} = \frac{\Delta P}{\eta \cdot (R_m + R_a)} \tag{5}$$

The resistance caused by the adsorbed solute on the membrane can be measured from Eqs. (4) and (5). In treating oil-water emulsions, the resistance caused by pore blocking (R_p) can be ignored due to the absence of particles. To simplify the resistance model, the gel-layer resistance (R_g) and concentration polarization (R_{cp})

are combined and expressed in R_{gcp}. The permeate flux at steady state, J_{ss}, becomes:

$$J_{ss} = \frac{\Delta P}{\eta \cdot (R_m + R_a + R_g + R_{cp})} = \frac{\Delta P}{\eta \cdot (R_m + R_a + R_{gcp})} \tag{6}$$

R_{gcp} can be determined once the values of R_m and R_a are known.

Flux Decline Model

The relation of the flux with time was investigated. Weisner and Aptel (24) proposed flux decline expressions caused by various mechanisms. Among these expressions, a model based on the concentration polarization and the adsorptive pore fouling mechanisms was used because it fits the experimental data very well. The mathematical model is expressed as:

$$J = Be^{-Kt} + J_{ss} \tag{7}$$

where J_{ss} is steady-state permeate flux and K indicates the rate constant toward the concentration polarization and/or adsorptive pore fouling phenomena. By applying the boundary conditions: $J = J_o$ @ $t = 0$, and $J = J_{ss}$ @ $t = \infty$, Eq. (7) can be rewritten as:

$$J = (J_o - J_{ss})e^{-bt} + J_{ss} \tag{8}$$

where J_o is the flux at initial time ($t = 0$).

RESULTS AND DISCUSSION

Calibration Curve of Kerosene

The UV-VIS absorption spectra in Fig. 2a indicated that there were two maximum absorption peaks within the range of the scanned wavelength. One occurred at 219 nm and the other at 266 nm wavelength. Although the former peak yielded maximum absorption, its corresponding λ_{max} changed with the kerosene concentration and the absorbance did not respond linearly with respect to the oil concentration. The absorbance at 266 nm was better for quantification and the calibration curve is shown in Fig. 2b. The coefficient of determination (R^2) of

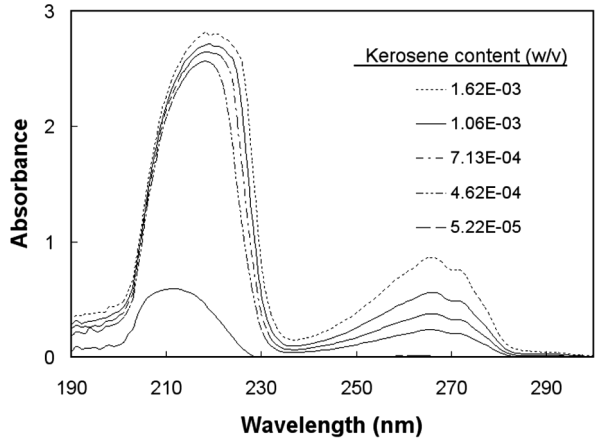

(a)

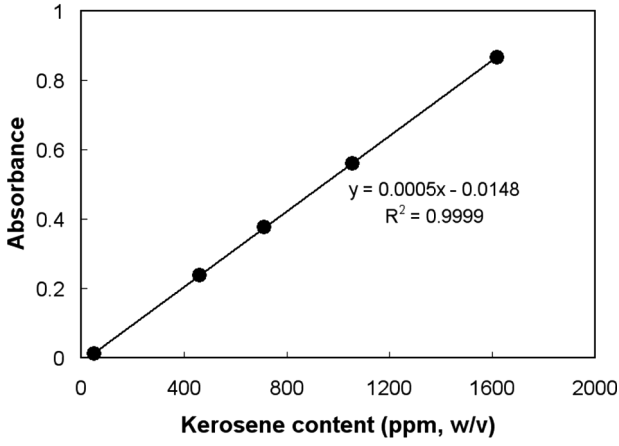

(b)

Figure 2. UV-ViS absorption spectra (a) and calibration curve (b).

0.9999 indicated an excellent linearity. This calibration curve was used for the determination of the permeate oil content.

Effect of Trans-Membrane Pressure (ΔP) on Permeate Flux

The pure water permeation flux was measured at various trans-membrane pressures, as shown in Fig. 3. The water permeability was calculated to be $6.55 \pm 0.28 \times 10^{-5}\,\mathrm{m^3/m^2\,s}$ bar, which is typical in a

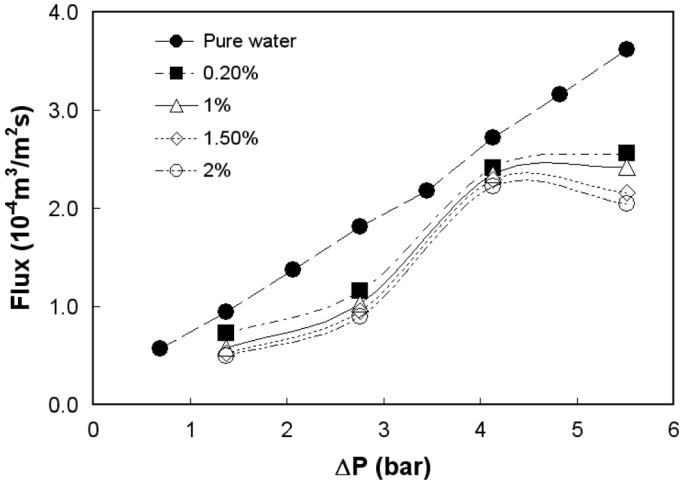

Figure 3. The relationship between the initial permeate flux and various trans-membrane pressures when fed with different oil content (feed velocity: 0.587 m/s, temperature: 20°C).

MF process (25). A feed containing 0.2–2% oil was fed into the membrane module. The relationship between the initial permeate flux with various trans-membrane pressure is shown in Fig. 3. The permeate flux was increased with the pressure until a plateau was reached. It can be explained that the higher trans-membrane pressure results in water droplets to pass rapidly through the membrane pores. However, concentration polarization occurs at high trans-membrane pressure and the increase of the driving force was off-set by the resistance formed in the boundary layer. Figure 3 indicates that ΔP of 4.14 bar (60 psi) was optimal in this process. Increasing the pressure further did not benefit the operation. Therefore, the operating pressure was kept at 4.14 bar throughout the remaining experiments. The corresponding flux under this operating pressure was expressed as limiting flux and used in the calculation shown in the next section.

Estimation of Mass Transfer Coefficient

The concentration polarization model was used to describe the initial flow behavior with various oil-water emulsions. By plotting the limiting flux (J_∞) vs. the natural log of the oil concentration, a slope value corresponding to the mass transfer coefficient (k) can be obtained (25). The data indicates that the k was 2.687×10^{-5} m/s. From the Deissler

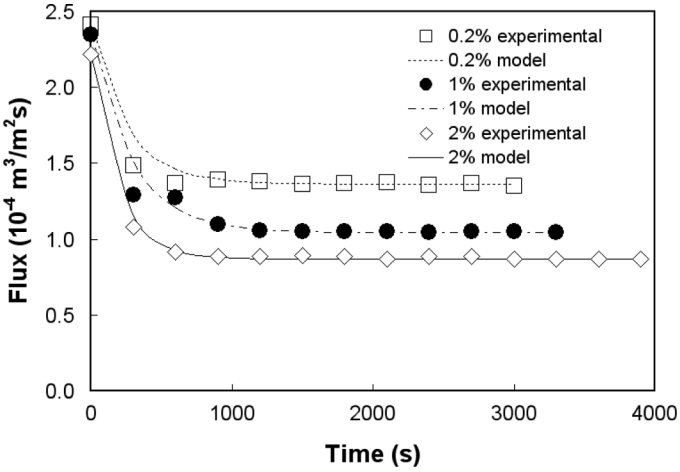

Figure 4. Flux decline of various oil-water emulsions (Trans-membrane pressure: 4.14 bar, feed velocity: 0.587 m/s, temperature: 20°C).

dimensionless equation for turbulent flow (25), the diffusion coefficient (D) was found to be $9.765 \times 10^{-10}\,m^2/s$. The boundary layer thickness (δ) was calculated to be $3.634 \times 10^{-5}\,m$.

Flux Decline of Oil-Water Emulsion at Various Oil Contents

Figure 4 shows the flux decline in the oil-water emulsion with oil content 0.2–2%. The data indicates that the decrease in oil concentration produces an increase in both the initial and final flux values. The permeate flux decreased with filtration time during the development of the fouling layer. Once the fouling layer was established, the permeate flux became constant for a given set of experimental conditions. The flux decreased rapidly in the first 5 minutes and remained unchanged after 10 minutes of operation. Comparing the flux pattern with the flux decline expressions caused by various mechanisms proposed by Weisner and Aptel (24), it was concluded that the flow decline was resulted mainly from concentration polarization and/or adsorptive pore fouling. These two mechanisms are characterized by a steady-state flux after a certain time, whereas the flux constantly decreased with time in the case where cake formation or pore blockage occurred. Table 2 summarizes the effects of oil concentration on the initial flux (J_o) and steady-state flux (J_{ss}). Both data sets decreased with increasing oil concentration in the feed.

Table 2. The effect of oil concentration on J_o and J_{ss}

Oil concentration (%)	J_o ($10^{-4}\,m^3/m^2\,s$)	J_{ss} ($10^{-4}\,m^3/m^2\,s$)	J_{wa} ($10^{-4}\,m^3/m^2\,s$)
0.2	2.62	1.47	1.50
0.5	2.59	1.37	1.40
1.0	2.35	1.04	1.23
1.5	2.29	1.00	1.16
2.0	2.22	0.86	1.11

Trans-membrane pressure: 4.14 bar, feed velocity: 0.587 m/s, temperature: 20°C.

With an oil-water emulsion concentration, the data of J_o, J_{ss}, and the flux between them were used to fit Eq. (8) and the value of b was determined. The results for the b value ranged from 3.377×10^{-3} to $5.248 \times 10^{-3}\,s^{-1}$. Figure 4 shows the comparison of experimental and the model fitted data. The model described the flow decline sufficiently.

Resistance-In-Series Model

The pure water flux through the clean membrane was about $2.708 \times 10^{-4}\,m^3/m^2s$ at a trans-membrane pressure of 4.14 bar, and the hydrodynamic resistance of the membrane was calculated as $1.53 \times 10^{12}\,m^{-1}$ using Eq. (4). Figure 5 shows the extent of steady-state pure water flux decrease in the membrane which had oil adsorption on the membrane surface. The adsorbed oil layer caused pure water flux reduced by 40–60%, depending on the oil concentration.

The cross-sectional views on the ceramic membrane were examined under scanning electron microscope. The clean membrane showed smooth top layer (Fig. 6a) and the oil-adsorbed membrane exhibited a rough surface (Fig. 6b). After cleaning, the oily surface became even and smooth again. This finding confirm the oily layer possessed additional resistance and hindered water transport.

Table 3 summarizes the individual resistance contributed to the flux decline as partitioned into R_m, R_a, and R_{gcp} which were calculated using Eqs (4)–(6). It indicates that the oil (solute) adsorption on the membrane surface was a major source of resistance. The adsorption resistance ranged from $1.23 \times 10^{12}\,m^{-1}$ to $2.20 \times 10^{12}\,m^{-1}$ as the oil concentration increased from 0.2 to 2.0% (Table 3). As the oil content in the feed increased, the gel formation and concentration polarization played

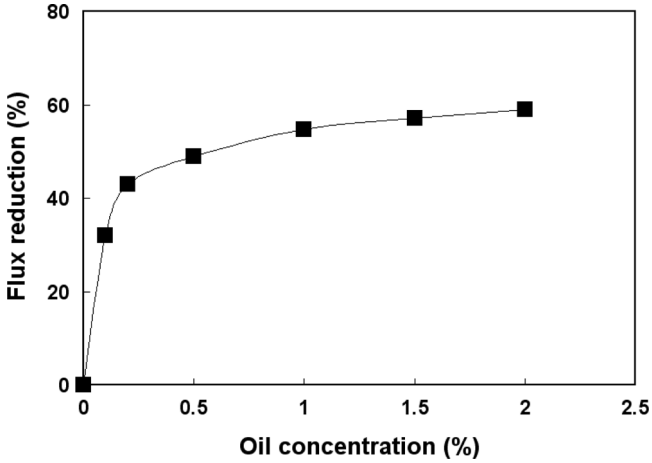

Figure 5. Pure water flux reduction after oil adsorption on membrane surface (Trans-membrane pressure: 4.14 bar, feed velocity: 0.587 m/s, temperature: 20°C).

a more significant role. The resistance values found in this study are comparable to and in the same order as those reported in the ultrafiltration of oil-in-water emulsions on ceramic membranes of 50- and 300-kDa molecular weight cut-off by Lobo et al. (26). In the filtration of 1% oil emulsion they summarized that the adsorption resistance was in the range of $0.33 \times 10^{12}\,m^{-1}$ and $5.27 \times 10^{12}\,m^{-1}$ for velocity ranging from 2.5 to 4.2 m/s and the pH varied between 3 and 9. In the ultrafiltration of apple juice using 30- or 300-kDa molecular weight cut-off ceramic membranes at 100 kPa, Vladisavljevic et al. (27) found higher resistance values ($2 \times 10^{13}\,m^{-1}$ to $6 \times 10^{13}\,m^{-1}$) from the overall fouling resistance exerted by the solids present in the juice, which corresponds to the sum of R_a and R_{gcp} in this study.

Since oil adsorption played an important role in the flux decline, we can further examine its mechanism during the filtration process. It is assumed that a reversible adsorption occurred in the process. That is, the dispersed oil can be adsorbed onto the membrane surface and form a gel layer. Conversely, the gel layer can be dispersed as oil droplets into the aqueous phase. The relationship between these two states is expressed in the following equation:

$$dispersed\ oil \longleftrightarrow oil\ gel\ layer \tag{9}$$

The forward and backward reaction rate constants are assumed to be k_1 and k_2, respectively. The oil gel lager amount as a function of time

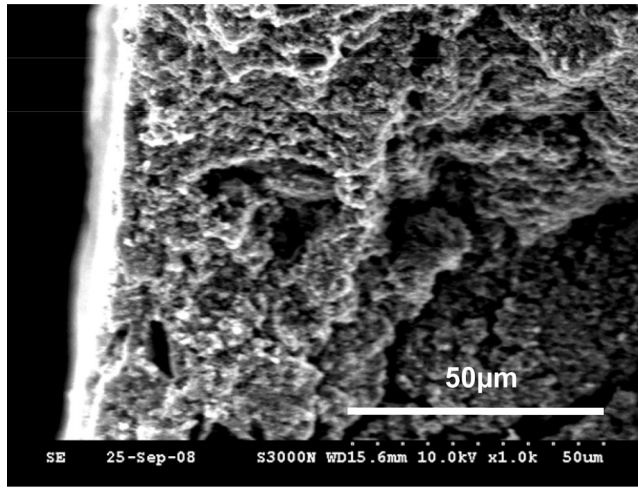

(a)

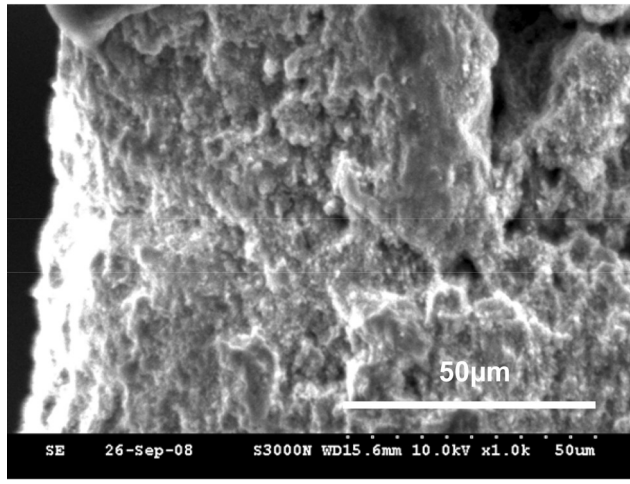

(b)

Figure 6. Scanning electron micrograms of (a) pristine ceramic membrane, and (b) membrane immersed in 5% kerosene emulsion for three days.

is shown in the following equation:

$$[oil\ gel\ layer] = \frac{k_1}{k_1 + k_2}\{1 - \exp[-(k_1 + k_2)t]\}[dispersed\ oil]_0 \qquad (10)$$

Since flux decline is related to the gel layer thickness, the flux decline with time is associated with the gel layer deposition rate on the membrane

Table 3. Individual resistance contributed to flux decline

Oil concentration in feed (%)	R_m ($10^{12}\,m^{-1}$)	R_a ($10^{12}\,m^{-1}$)	R_{gcp} ($10^{12}\,m^{-1}$)
0.2	1.53	1.23	0.06
0.5	1.53	1.42	0.07
1.0	1.53	1.85	0.58
1.5	1.53	2.03	0.65
2.0	1.53	2.20	1.09

Trans-membrane pressure: 4.14 bar, feed velocity: 0.587 m/s, temperature: 20°C.

surface during the time course. Eq. (8) can be rearranged as the following equation:

$$J = J_0 + J_{ss}(1 - \exp(-bt)) \tag{11}$$

Comparing Eqs. (10) and (11), one can obtain the sum of the rate constants ($k_1 + k_2$) as equal to b value. Therefore the ($k_1 + k_2$) value also ranged from 3.377×10^{-3} to $5.248 \times 10^{-3}\,s^{-1}$. In addition, the ratio of J_{ss}/J_0 is equal to $k_1/(k_1 + k_2)$, which was in the range of 39% to 56% in this study. Combining the data of ($k_1 + k_2$) and $k_1/(k_1 + k_2)$, one can solve for k_1 and k_2. The results were $(1.93 \pm 0.34) \times 10^{-3}\,s^{-1}$ for k_1 and $(2.28 \pm 0.80) \times 10^{-3}\,s^{-1}$ for k_2, respectively. The analysis above demonstrates that the flux decline can be explained using the simplified mechanism of reversible adsorption of the oil component onto the membrane surface.

Effect of Temperature on Flux

The feed temperature was increased from 20°C to 40 and then to 60°C to study the temperature effect. The results show that increasing the temperature increased both the initial flux (J_o) and the flux at steady state (J_{ss}). The temperature effect on the flux was significant ($p < 0.001$) as indicated by the statistical analysis of variance. The flux increase at a higher temperature can be explained in a lower viscosity. Equations (4)–(6) demonstrate that the water flux was inversely proportional to the solution viscosity. The temperature effect can be expressed by the Arrhenius equation (Fig. 7) and an activation energy of 2.918 kJ/mol was determined for steady state flux from 1% oily water.

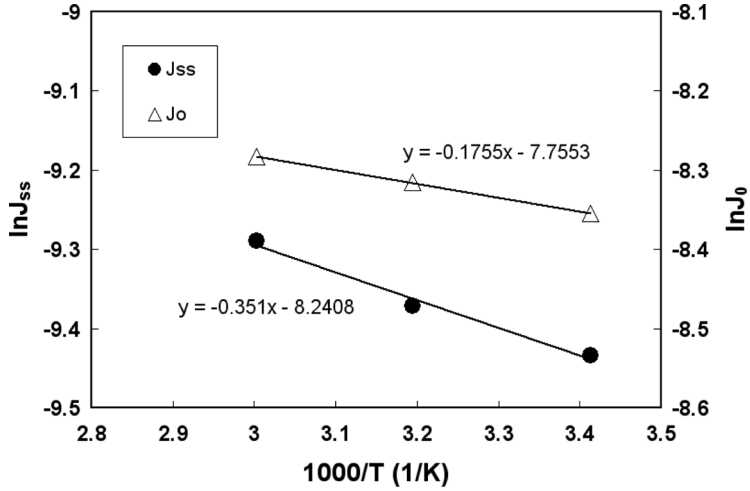

Figure 7. Arrhenius plots of initial flux (J_o) and steady state flux (J_{ss}) as a function of reciprocal of temperature for 1% oily water.

Oil Retention at Various VCF

The kerosene-water emulsions were concentrated in a batch operation. The average oil retention was measured by sampling the permeate at a predetermined VCF. Table 4 shows the oil retention at various feed concentrations. The oil retention was higher with lower oil content in the feed. The average oil retention in the feed containing 0.5% oil was

Table 4. Oil content of permeate and oil retention at different volume concentration factors (VCF[‡]) of feed of 0.2%, 0.5%, and 1.5% oil content[§]

	Oil content of permeate (ppm, v/v)				Retention (%)			
Feed \ VCF	1.5	2	3	4	1.5	2	3	4
0.2%	ND*	ND*	ND*	4.4	>99.9	>99.9	>99.9	99.8
0.5%	32	39	37	34	99.8	99.6	99.5	99.5
1.5%	2932	3558	4336	7512	93.5	88.1	80.7	62.4

*ND: not detectable.
†Oil retention $= (1 - V_P C_P / V_F C_F) \times 100\%$.
‡VCF = initial feed volume/final volume.
§Trans-membrane pressure: 4.14 bar, feed velocity: 0.587 m/s, temperature: 20°C.

99.5% at a volume concentration factor of 4. As the emulsion became more concentrated, the oil retention decreased.

Table 5. Filtration efficiency comparison on literature data

Membrane	Pore size (μm) or molecular weight cut-off (MWCO)	Feed concentration (10^3 ppm) (Temperature)	Permeance (10^{-6} m^3/m^2s bar)	Reference
Polyethersulfone	NA[a] (UF range)	100 (25°C)	1.5–4.6	5
Polymeric	1–5 kD	5 (35°C)	1.0–3.2	14
	20–30 kD		4.1–6.5	
	60–100 kD		15–24.5	
Polysulfone	MWCO of 30 kD	0.1 – 0.4 (25°C)	6.39–10.60	6
2-Hydroxyethyl methacrylate coated polysulfone	MWCO of 300 kD	0.4 (25°C)	8.17	8
Surface-modified polyacrylonitrile	0.1	10 (40°C)	2.78	13
Polysulfone	0.1	1 (22°C)	7.03	16
Polyvinylidene-fluoride	0.45	1 (22°C)	18.80	16
Zirconia-based membrane grafted with 10–30% polyvinylpyrro-lidone	MWCO of 10.3 kD	34.3 (27°C)	1.25–1.30	7
Zirconia on carbon support	MWCO of 15 kD	34.3 (27°C)	1.62	7
Zirconia on carbon support	MWCO of 300 kD	1–5 (18°C)	48.60 – 0[b]	2
Zirconia coated inorganic membrane	0.1	1 (22°C)	8.89	16
α-Alumina ceramic	0.2	10 (40°C)	6.94	13
NaA/α-Al_2O_3	1.2	0.1	10	20
	0.4		1.39	
Zirconia/titania on carbon support	0.14	2–15 (20°C)	33.60 – 21.70	This work

[a]Not available.
[b]Almost no water flux at 5000 ppm.

Wu et al. (9) pointed out the mean particle size of oil droplets in the surfactant-free aqueous solution was 0.36 μm at 1% oil content. However, the droplets exhibited a broad particle size distribution; about 10% were less than 0.1 μm (9). Theoretically the use of this 0.14-μm filtration membrane would be able to retain at least 80% of the oil droplets in water, without showing dependence on the oil concentration, if the oil droplets had behaved like hard spheres. In a real situation, the adsorbed oil on the separation layer may form a gel layer. This gel layer thickness increases with the oil concentration. At the high oil level, such as 1.5%, oil breakthrough became significant under the shear force exerted by the applied pressure. The oil droplets might be deformed and extruded through the pores and leached out into the permeate stream. The retention ratio was reduced considerably under this circumstance (Table 4).

Comparison with Literature Data

The results from this work were compared with other studies as shown in Table 5. A general trend for the permeate flux was an increase with the increases in the pore size and a decrease with the increase in oil concentration. Table 5 clearly demonstrated that superior flux permeance was obtained ($2.17–3.36 \times 10^{-5}\ m^3/m^2\ s\ bar$ or $78–121\ L/m^2\ h\ bar$) using this microporous ceramic membrane, significantly higher than that for other membranes, taking into account the high oil content. This ceramic material is especially suitable for the microfiltration of emulsions containing oil concentrations less than 1.5%. At higher oil contents, membranes with smaller pore sizes are recommended to achieve similar oil rejection efficiency.

CONCLUSIONS

The flux decline and oil retention were studied on the microfiltration of kerosene-water mixtures using a tubular ceramic membrane. Under turbulent conditions, the flux decreased 50% from the initial flux. The mathematical equation $J = (J_o - J_{ss})e^{-bt} + J_{ss}$ could describe the flow decrease sufficiently. The solute diffusion coefficient was $9.765 \times 10^{-10}\ m^2/s$ and the mass transfer coefficient was $2.687 \times 10^{-5}\ m/s$ in this system. The resistance-in-series model was applied to describe the flux decline. The resistance caused by oil adsorption on the membrane surface governed the steady-state flux (J_{ss}). However, gel formation and concentration polarization also became significant as the oil concentration increased.

Nevertheless, this ceramic membrane exhibited higher water permeability than other membranes as reported in the literature. For oily water containing less than 0.5% kerosene content, the steady-state permeate flux of $3.36 \times 10^{-5}\,m^3/m^2\,s$ bar ($121\,L/m^2\,h$ bar) could be achieved and the oil retention was as high as 99.5% at a volume concentration factor of 4. A reversible model of dispersed oil adsorption into the gel state was used to explain the flux decline during the filtration process.

ACKNOWLEDGEMENT

The authors wish to express their gratitude to Chang Gung University (UERPD 270161) for its financial support. Valuable discussion with the Referees is greatly acknowledged.

REFERENCES

1. EPA Taiwan ROC. (1997) *Effluent Standards*. EPA Taiwan: Taipei, ROC, No: 0060.
2. Elmaleh, S.; Ghaffor, N. (1996) Cross-flow ultrafiltration of hydrocarbon and biological solid mixed suspensions. *J. Membr. Sci.*, *118*: 111–120.
3. Lee, S.; Aurelle, Y.; Roques, H. (1984) Concentration polarization, membrane fouling and cleaning in ultrafiltration of soluble oil. *J. Membr. Sci.*, *19*: 23–38.
4. Vigo, F.; Uliana, C.; Cavazza, B.; Salvemini, F. (1984) Mechanical, chemical and bacterial resistance of modified polyvinylidene fluoride membranes suitable for ultrafiltration of oily emulsions. *J. Membr. Sci.*, *21*: 295–306.
5. Hamza, A.; Pham, V.A.; Matsuura, T.; Santerre, J.P. (1997) Development of membranes with low surface energy to reduce the fouling in ultrafiltration applications. *J. Membr. Sci.*, *131*: 217–227.
6. Mohammadi, T.; Kohpeyma, A.; Sadrzadeh, M. (2005) Mathematical modeling of flux decline in ultrafiltration. *Desalination*, *184*: 367–375.
7. Faibish, R.S.; Cohen, Y. (2001) Fouling-resistant ceramic-supported polymer membranes for ultrafiltration of oil-in-water microemulsions. *J. Membr. Sci.*, *185*: 129–143.
8. Song, K.H.; Lee, K.R. (2007) Treatment of oily wastewater using membrane with 2-hydroxyethyl methacrylate-modified surface. *Korean J. Chem. Eng.*, *24*: 116–120.
9. Wu, C.; Li, A.; Li, L.; Zhang, L.; Wang, H.; Qi, X.; Zhang, Q. (2008) Treatment of oily water by a poly(vinyl alcohol) ultrafiltration membrane. *Desalination*, *225*: 312–321.
10. Bodzek, M.; Konieczny, K. (1992) The use of ultrafiltration membranes made of various polymers in the treatment of oil-emulsion wastewaters. *Waste Manage*, *12*: 75–84.

11. Keurentjes, J.T.F.; Doornbusch, G.I.; Van't Riet, K. (1991) The removal of fatty acids from edible oil. Removal of the dispersed phase of a water-in-oil dispersion by a hydrophilic membrane. *Sep. Sci. Technol.*, *26* (3): 409–423.
12. Mueller, J.; Cen, Y.; Davis, R.H. (1997) Crossflow microfiltration of oily water. *J. Membr. Sci.*, *129*: 221–235.
13. Zaidi, A.; Simms, K.; Kok, S. (1992) The use of micro/ultrafiltration for the removal of oil and suspended solids from oilfield brines. *Water Sci. Technol.*, *25*: 163–176.
14. Peng, H.; Tremblay, A.Y. (2008) The selective removal of oil from wastewaters while minimizing concentrate production using a membrane cascade. *Desalination*, *229*: 318–330.
15. Mavrov, V.; Mavrova, Zh.; Georgieva, V.; Bonev, B. (1991) Condensate re-use by ultrafiltration oil removal. *Desalination*, *83*: 195–207.
16. Koltuniewicz, A.B.; Field, R.W.; Arnot, T.C. (1995) Cross-flow and dead-end microfiltration of oily-water emulsion. Part I: experimental study and analysis of flux decline. *J. Membr. Sci.*, *102*: 193–207.
17. Koltuniewicz, A. B.; Field, R.W. (1996) Process factors during removal of oil-in-water emulsions with cross-flow microfiltration. *Desalination*, *105*: 79–89.
18. Hsieh, H.P.; Liu, P.K.T.; Dillman, T.R. (1991) Microporous ceramic membranes. *Polym. J.*, *23*: 407–415.
19. Hua, F.L.; Wang, Y.J.; Tsang, Y.F.; Chan, S.Y.; Sin, S.N.; Chua, H. (2007) Study of microfiltration behaviour of oily wastewater. *J. Environ. Sci. Health, Part A: Toxic/Hazard. Subst. Environ. Eng.*, *42*: 489–496.
20. Cui, J.; Zhang, X.; Liu, H.; Liu, S.; Yeung, K.L. (2008) Preparation and application of zeolite/ceramic microfiltration membranes for treatment of oil contaminated water. *J. Membr. Sci.*, *325*: 420–426.
21. Belfort, G.; Davis, R.H.; Zydney, A.L. (1994) The behavior of suspensions and macromolecular solutions in crossflow microfiltration. *J. Membr. Sci.*, *96*: 1–58.
22. Mulder, M.H.V. (1995) Polarization Phenomena and Membrane Fouling. In: *Membrane Separations Technology. Principles and Applications*, Noble, R.D.; Stern, S.A. eds.; Elsevier: Amsterdam, 45–84.
23. Gu, H.; Chen, G.; Xu, N.; Qi, W. (1998) Determination of oil content in oily wastewater from steel works by CPA-ultraviolet spectrophotometry. *Petrochem. Technol. (Chinese)*, *27*: 356–360.
24. Wiesner, M. R.; Aptel, P. (1996) Mass transport and permeate flux and fouling in pressure-driven processes. In: *Water Treatment Membrane Processes*, Mallevialle, J.; Odendaal, P.E.; Wiesner, M.R., eds.; McGraw-Hill Co.: New York, Ch. 4.
25. Mulder, M. (1996) *Basic Principles of Membrane Technology;* 2nd Ed.; Kluwer Academic Publishers: Boston, USA.
26. Lobo, A.; Cambiella, Á.; Benito, J.M.; Pazos, C.; Coca, J. (2006) Ultrafiltration of oil-in-water emulsions with ceramic membranes: Influence of pH and crossflow velocity. *J. Membr. Sci.*, *278*: 328–334.
27. Vladisavljevic, G.T.; Vukosavljevic, P.; Bukvic, B. (2003) Permeate flux and fouling resistance in ultrafiltration of depectinized apple juice using ceramic membranes. *J. Food Eng.*, *60*: 241–247.